5

Two experimental laws of fully developed turbulence

Experimental data will now be presented to illustrate two basic empirical laws of fully developed turbulence.

(i) **Two-thirds law.** *In a turbulent flow at very high Reynolds number, the mean square velocity increment* $\langle(\delta v(\ell))^2\rangle$ *between two points separated by a distance* ℓ *behaves approximately as the two-thirds power of the distance.*[1]

(ii) **Law of finite energy dissipation.** *If, in an experiment on turbulent flow, all the control parameters are kept the same, except for the viscosity, which is lowered as much as possible, the energy dissipation per unit mass* dE/dt *behaves in a way consistent with a finite positive limit.*

These laws seem to hold, at least approximately, for almost any turbulent flow. Let us now examine examples of such data.

5.1 The two-thirds law

Fig. 5.1 shows a log–log plot of the *second order longitudinal structure function*

$$S_2(\ell) \equiv \left\langle\left(\delta v_\parallel(\ell)\right)^2\right\rangle. \tag{5.1}$$

The measurement was done in the S1 wind tunnel of ONERA.[2]

It is seen that there is a substantial $\ell^{2/3}$ range. Let us be somewhat more specific now. The *longitudinal velocity increment* is defined as

$$\delta v_\parallel(\boldsymbol{r},\boldsymbol{\ell}) \equiv [\boldsymbol{v}(\boldsymbol{r}+\boldsymbol{\ell}) - \boldsymbol{v}(\boldsymbol{r})]\cdot\frac{\boldsymbol{\ell}}{\ell}, \tag{5.2}$$

[1] With restrictions on the range of variation of ℓ which will be given later.

[2] All the data from S1 reported in this book have been obtained by Y. Gagne, E. Hopfinger and M. Marchand.

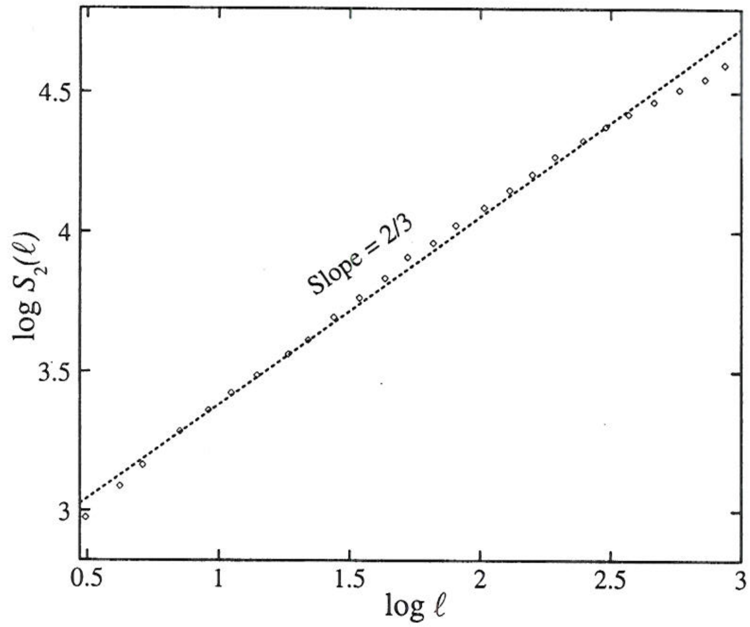

Fig. 5.1. log–log plot of the second order structure function in the time domain for data from the S1 wind tunnel of ONERA. Courtesy Y. Gagne and E. Hopfinger.

where $\ell = |\boldsymbol{\ell}|$. Thus $\delta v_{\|}(\boldsymbol{r}, \boldsymbol{\ell})$ is the velocity increment between two points separated by $\boldsymbol{\ell}$, projected onto the line of separation. When the turbulence is homogeneous and isotropic, we can unambiguously drop the dependence on $\boldsymbol{r}$ in the second order moment $\langle(\delta v_{\|}(\boldsymbol{r}, \boldsymbol{\ell}))^2\rangle$ and use ℓ instead of $\boldsymbol{\ell}$ as is done in (5.1). The wind tunnel S1 is shown on Fig. 5.2. It is over 150 m long. The widest part, known as the return duct, has a circular cross section with a diameter of 24 m. A hot wire probe was suspended near the point marked 'M'. It recorded the streamwise (parallel to the mean flow) component of the velocity. The averaging for the data shown in Fig. 5.1 is a time average, using ergodicity (Section 4.4). The mean flow velocity was 20 m/s. The Reynolds number based on this mean flow and the diameter of the duct was about 3×10^7. The Reynolds number based on the r.m.s. velocity and the integral scale (around 15 m) was about 1.5×10^6. The r.m.s. velocity fluctuations represent about 7% of the mean flow.

This relatively small ratio, the *turbulence intensity*, typical of wind tunnels, justifies the use of the *Taylor hypothesis*,[3] as now explained. Let

[3] From G.I. Taylor, the Cambridge fluid dynamicist.

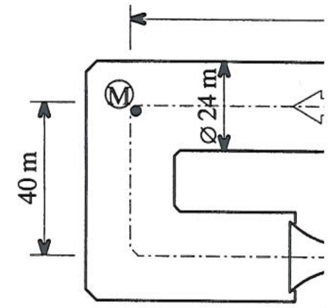

Fig. 5.2. The S

us denote by $v'(t,x)$ the velocit
of reference of the mean flow.
In the frame of reference of th

$$v(t,x) =$$

where U is the mean flow. If we
I is given by

$$I =$$

it is easily checked that most
from the spatial argument $x -$
the temporal variation of v at
variation of v'. The correspon
and temporal increments τ for

Most experimental data on f
the time domain and then rec
hypothesis. The time (or freq
position (or wavenumber) axis.
indicate in figure captions whe
domain or in the space domain
The question of how the Ta

[4] Attention has to be paid to the fact

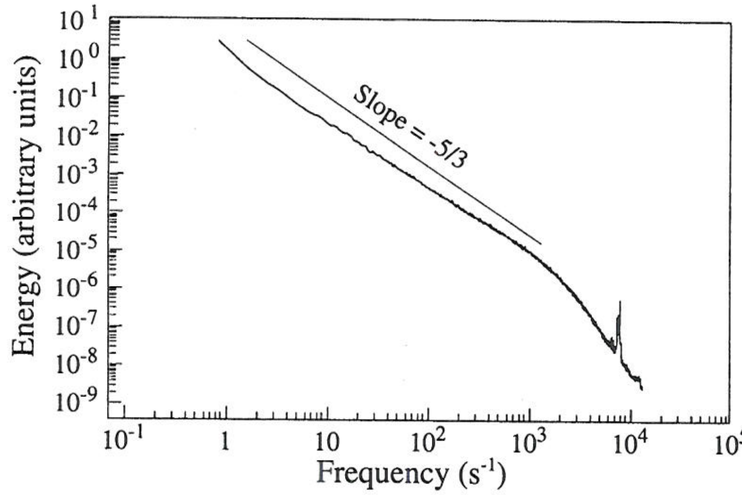

Fig. 5.4. Energy spectrum in the time domain for data from S1. Reynolds number $R_\lambda = 2720$. Courtesy Y. Gagne and M. Marchand.

law over a suitable range. The larger the Reynolds number, the wider this range.

Fig. 5.4 shows the energy spectrum for the best data obtained so far from the S1 wind tunnel. This is again a log–log plot. The horizontal axis is a frequency which can be reinterpreted as a wavenumber by use of the Taylor hypothesis. A power-law scaling k^{-n} with an exponent n close to 5/3 is observed over a very substantial range of about three decades of wavenumber. This range is called the *inertial range*, a name which will be justified in Section 6.2.5.

The features shown in Fig. 5.4 need some comment. First, there is a narrow spike in the spectrum at high wavenumbers. This is probably due to a mechanical vibration which is hard to avoid when a scientific experiment is set up temporarily in a major industrial facility such as S1. Second, it is not known if the discrepancy from a pure 5/3-law is significant (a straight line of slope $-5/3$ is shown for comparison).[7] Third, it should be noticed that the range of wavenumbers over which scaling holds for $E(k)$ is much larger than the range of distances over which scaling holds for $S_2(\ell)$. As observed by M. Nelkin (private communication, 1988), the fact that the two functions are, by (4.53), essentially Fourier transforms of each other does not imply identical spans of

[7] When a power-law is fitted to the data, the value of the exponent changes somewhat with the choice of the fitting region.

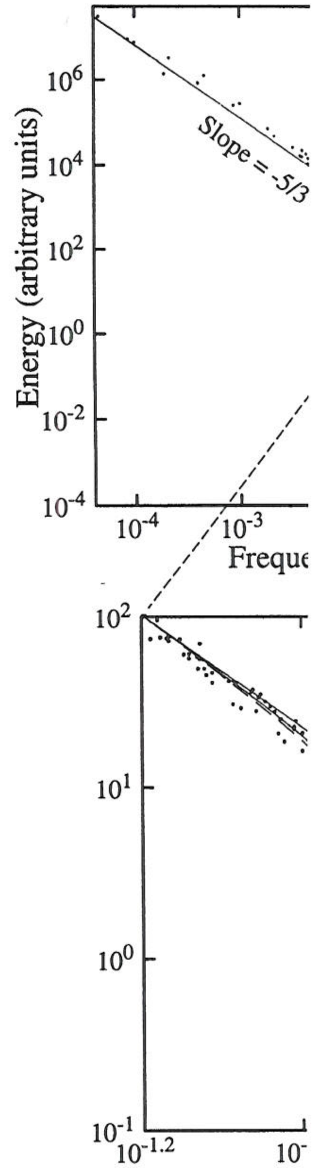

Fig. 5.5. log–log plot of the energy sp
of the beginning of the dissipation r
and Moilliet 1962).